

Scalable, Divergent Synthesis of a High Aspect Ratio Carbon Nanobelt

Harrison M. Bergman, Gavin R. Kiel, Rex C. Handford, Yi Liu, and T. Don Tilley*



Cite This: *J. Am. Chem. Soc.* 2021, 143, 8619–8624



Read Online

ACCESS |

Metrics & More

Article Recommendations

Supporting Information

ABSTRACT: Carbon nanobelts are molecules of high fundamental and technological interest due to their structural similarity to carbon nanotubes, of which they are molecular cutouts. Despite this attention, synthetic accessibility is a major obstacle, such that the few known strategies offer limited structural diversity, functionality, and scalability. To address this bottleneck, we have developed a new strategy that utilizes highly fused monomer units constructed via a site-selective [2 + 2 + 2] cycloaddition and a high-yielding zirconocene-mediated macrocyclization to achieve the synthesis of a new carbon nanobelt on large scale with the introduction of functional handles in the penultimate step. This nanobelt represents a diagonal cross section of an armchair carbon nanotube and consequently has a longitudinally extended structure with an aspect ratio of 1.6, the highest of any reported nanobelt. This elongated structure promotes solid-state packing into aligned columns that mimic the parent carbon nanotube and facilitates unprecedented host–guest chemistry with oligo-arylene guests in nonpolar solvents.

Molecular belts have fascinated chemists for many years, given their unusual structures, challenging syntheses, and potential to display unique optoelectronic and supramolecular properties.^{1,2} This interest has led to the synthesis of a wide range of belt-like structures, including hydrocarbon belts,^{3,4} heteroatom-doped belts,^{5–9} porphyrin belts and nanotubes,^{10,11} conjugated belts such as the Schlüter¹² and Gleiter belts,¹³ and recently phenine nanotubes.^{14,15} Carbon nanobelts (CNBs), defined as a closed loop of fully fused benzene rings with a radial π system, are perhaps the best known subclass of molecular belts and have been of great fundamental interest to the organic community for over 60 years. Speculation on the possible existence of CNBs dates back to at least 1954, when Heilbronner proposed [12]-cyclacene as a highly distorted, radial π system with potentially interesting electronic properties;¹⁶ however, this structure has yet to be prepared.^{17,18} This early proposal kindled interest in other types of CNBs such as cyclophenacene and the Vögtle belt,¹⁹ but these macrocycles have also eluded isolation. The discovery of carbon nanotubes in 1991 heightened interest in cyclic nanocarbons,²⁰ since they represent well-defined, molecular cutouts of the nanotubes and should retain some properties of the parent tubular structure. They could also offer synthetic entry points for the bottom-up synthesis of single-walled carbon nanotubes.^{21–23} Redoubled efforts to prepare CNBs^{24,25} led to a partially hydrogenated C_{60} fullerene possessing an embedded [10]cyclophenacene.²⁶ Additionally, on the basis of matrix-assisted laser desorption ionization (MALDI), a cyclophenacene²⁷ and [8]cyclacene²⁸ have been observed.

The first example of an isolable, discrete CNB was described in Itami's landmark report in 2017 describing the synthesis of a [12]-armchair nanobelt (Figure 1a).²⁹ Shortly afterward, Itami published an optimized synthetic procedure that provided [16]- and [24]-armchair nanobelts.³⁰ In 2019, Miao described

a [24]-armchair nanobelt as well as the first chiral nanobelt.³¹ Finally, in 2020, Chi and Itami independently reported syntheses of the first zigzag carbon nanobelts.^{32,33} With these results, CNBs representing the three major classes of carbon nanotube structure—armchair, chiral, and zigzag—had finally been realized. Very recently, Miao reported the synthesis of a new class of zigzag CNBs representing a diagonal rather than a horizontal cross section of a carbon nanotube.³⁴

Despite the impressive advances of the past few years, current strategies for nanobelt synthesis are severely limited. The reported methods are uniformly low-yielding, give small quantities of product (≤ 22 mg), and provide limited opportunities for late-stage functionalization. Additionally, the structural diversity of reported CNBs is still low, particularly with respect to control over the length–width aspect ratio, which should have a profound impact on supramolecular properties. These limitations hinder the advancement of CNBs from fundamentally interesting structures to technologically relevant molecular materials.

The synthetic bottleneck is largely due to inherent challenges associated with the macrocyclization and ring-fusion steps, which suffer from high entropic penalties and many competing side reactions, while requiring the introduction of significant strain. Current strategies exacerbate these issues by relying on the assembly of several nonfused monomers during macrocyclization and the subsequent fusion

Received: April 21, 2021

Published: June 4, 2021



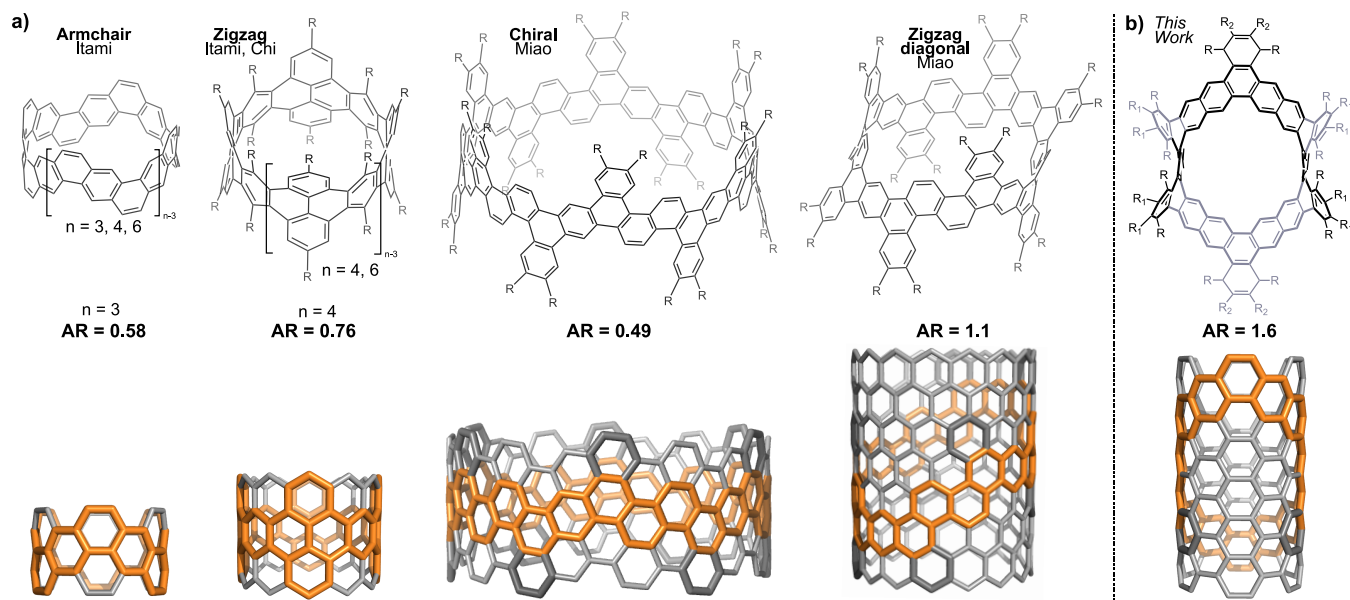
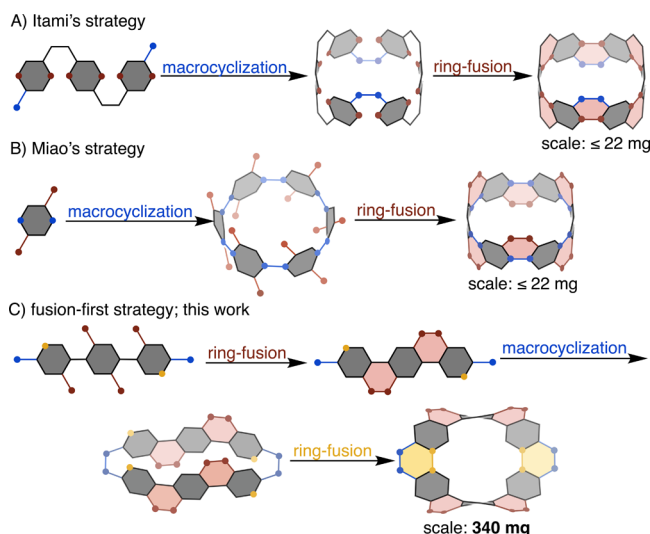


Figure 1. (a) Previously synthesized nanobelts of each major class and (b) the nanobelt synthesized in this work, illustrated chemically and as fragments of their parent carbon nanotube with length–width aspect ratio (AR) shown for each example.

of all rings in the final step to generate the nanobelt (Scheme 1a,b).

Scheme 1. Schematics of Key Strategies for Nanobelt Synthesis

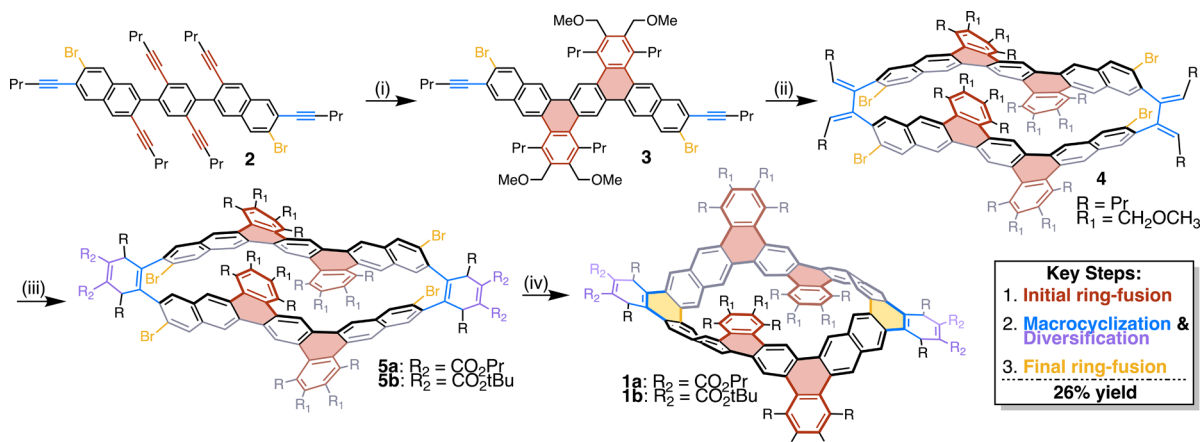


The synthetic strategy introduced in this report is designed to mitigate these challenges through the use of highly fused monomer units, which are then incorporated into a macrocycle requiring minimal further ring fusions to generate the nanobelt (Scheme 1c). By carrying out most of the requisite ring fusion early in the synthetic sequence, the building blocks employed for macrocyclization and ring fusion are “preorganized” and rigidified to minimize entropic penalties and deleterious side reactions. Zirconocene coupling of alkynes is utilized for macrocyclization, as this introduces linkages that provide the narrow bite angle ($\sim 60^\circ$) required to accommodate rigid, planar monomers into a macrocyclic framework. This new approach is demonstrated here in the synthesis of a new CNB in 26% yield (across the indicated key steps) on a 0.34 g scale,

which represents more than an order of magnitude increase in scale from previously reported CNBs. The ease of nanobelt functionalization is highlighted by diversification in the penultimate Diels–Alder cycloaddition step to generate a more soluble and crystalline nanobelt derivative. These nanobelts have a longitudinally extended structure representing a diagonal cross section of a [6,6] carbon nanotube (Figure 1b), giving them an aspect ratio of 1.6, the highest for any reported carbon nanobelt. This elongated tubular structure imbues the CNB with unique supramolecular behavior, including solid-state assembly into columnar arrays and complexation of unusual oligo-arylene guests in solution (*vide infra*).

The first key step was generation of a fully fused monomer unit, which was achieved by a site-selective Ir-catalyzed [2 + 2 + 2] cycloaddition^{35,36} of unfused precursor **2** in the presence of 4 equiv of 1,4-dimethoxy-2-butyne (Scheme 2). This produced monomer **3** in 81% yield on a 1.8 g scale. Importantly, **3** incorporates most of the necessary ring fusions for synthesis of the nanobelt, while preserving peripheral pentynyl and bromide groups utilized in the remaining coupling steps.

The diyne **3** was then used in an efficient macrocyclization via zirconocene coupling. The resulting zirconacyclopentadiene was hydrolyzed by *in situ* reaction with HCl to provide macrocycle **4** in 60% yield. Despite the introduction of 10 kcal/mol of strain energy (Scheme S2), this sequence does not require high dilution conditions, facilitating the isolation of this key intermediate on a gram scale. The syn-orientation of the bromides in **4** was confirmed by the presence of two distinct Cp resonances in the ¹H NMR spectrum of the intermediate zirconacyclopentadiene (Figure S1), which is crucial for success of the subsequent Yamamoto coupling. The exocyclic dienes formed by this macrocyclization procedure serve as a convenient synthetic handle for the late-stage introduction of nanobelt functionality via Diels–Alder cycloadditions, as demonstrated by syntheses of **5a** and **5b** in 86 and 85% yields, respectively.

Scheme 2. Synthesis of Longitudinally Extended Nanobelt **1**^a

These macrocycles were then subjected to a modified version of Stepien's conditions for ring fusion via Yamamoto coupling of the bromides³⁷ in 66 and 63% yield while building in 63 kcal/mol of strain energy (Page S21) to give nanobelts **1a** and **1b**. Thus, these nanobelts were accessed in 26% yield across the key steps shown. The efficient, high-yielding synthesis facilitated large-scale production of the nanobelts, with isolation of each on a 0.34 g scale. This represents a significant milestone for the chemistry of carbon nanobelts, as prior reported syntheses provide less than 23 mg.

Both nanobelts were structurally characterized by ^1H and ^{13}C NMR spectroscopy, matrix-assisted laser desorption/ionization (MALDI), and X-ray crystallography. The NMR spectroscopy revealed 5 and 20 non-equivalent aromatic protons and carbons, respectively, confirming its C_{2h} symmetry in solution, and the belt structure was unambiguously confirmed by X-ray crystallography. Suitable crystals of both **1a** and **1b** were grown by diffusion of hexamethyldisiloxane into THF solutions at -30°C , but the data for **1a** contains significant disorder (Figure S26). As shown in Figure 2a,b, **1b** has a long tubular belt structure, with a diameter across the center of 9.9 \AA and a length of 15.6 \AA from end to end of the core aromatic belt based on interatomic distances.

Strikingly, in the solid state, **1b** assembles into ordered columns with alignment of the nanobelt pores into a continuous channel (Figure 2c). This arrangement bears a great structural resemblance to the parent $[6,6]$ carbon nanotube of which **1b** is a molecular cutout (Figure 2d).

The photophysical and electronic properties of CNB **1b** were characterized by UV-vis absorption and emission spectroscopies (Figure S22) and cyclic voltammetry (Figures S23 and S24). The former revealed an absorption onset of 486 nm, corresponding to an optical HOMO–LUMO gap of 2.7 eV, while the latter provided an electrochemical HOMO–LUMO gap of 2.9 eV. The emission spectrum of **1b** displays a sharp maximum at 491 nm and a broad shoulder stretching to 600 nm.

While other belt-shaped macrocycles and cycloparaphenylanes have displayed a range of interesting supramolecular phenomena,³⁸ the host–guest chemistry of CNBs is still largely³⁹ unexplored. The unique tubular structure and unusual

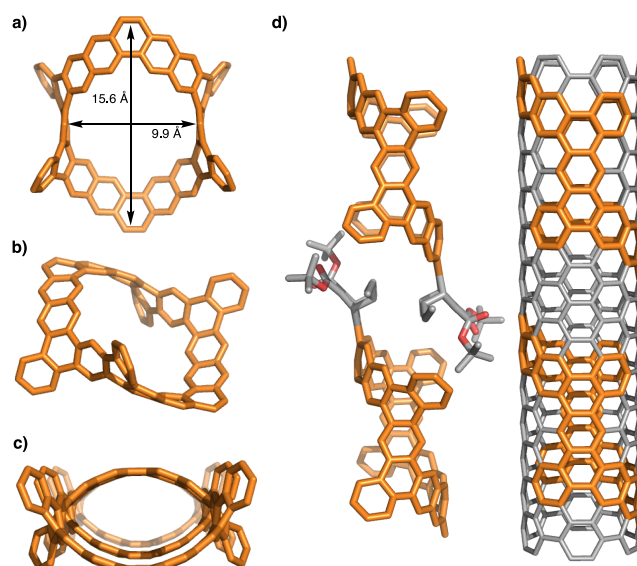


Figure 2. X-ray crystallographic structure of nanobelt **1b**. All side chains and solvent have been omitted for clarity, except where specified. (a) Top view; (b) side view; (c) view of solid-state packing along the *c* crystallographic axis highlighting pore alignment of the nanobelts; (d) view of packing along the *b* crystallographic axis highlighting the tubular arrangement and structural similarity to the parent $[6,6]$ carbon nanotube.

curvature of nanobelts **1a** and **1b** indicated that these macrocycles might function as effective hosts for a range of small molecules. **1b** was utilized for these studies due to its superior solubility. Several potential guests were examined by ^1H NMR spectroscopy by comparison of the chemical shifts of free guest with that of a 1:1 mixture of guest and nanobelt **1b**. While electron-poor guests such as TCNQ, octafluoronaphthalene, and methylviologen exhibited extremely small or no chemical shifts in the presence of **1b** (benzene-*d*₆ solution), aromatic guests *p*-terphenyl (pTP) and α -quaterthiophene (QT) showed modest but distinct chemical shifts suggesting interaction with the nanobelt **1b**.

While X-ray crystal structures of the host–guest complexes could not be obtained, both were DFT-optimized at the TPSS-

D3/def2-TZVP level to visualize the lowest energy conformations (Figure 3a,b).⁴⁰ These calculations indicate that

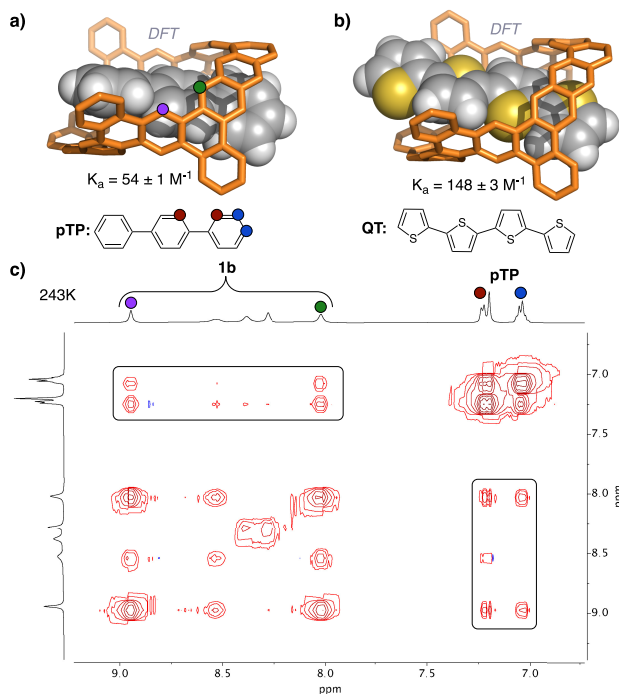


Figure 3. Host–guest chemistry of nanobelt **1b**. Computed structure of the (a) **1b**•pTP and (b) **1b**•QT complex optimized at the TPSS-D3/def2-TZVP level of theory; (c) NOESY NMR spectrum recorded at 243 K in THF-*d*₈ displaying correlations between pTP and **1b** resonances indicative of solution binding.

both pTP and QT bind to the inner cavity of the nanobelt in a 1:1 ratio, the enthalpic component of which appears to be driven by CH–π interactions and π–π stacking. Both QT and pTP displayed a single set of sharp peaks by ¹H NMR spectroscopy, indicating that complexation leads to dynamic behavior in the fast exchange regime at room temperature. Upon cooling a 1:1 mixture of **1b** and pTP to 243 K in THF-*d*₈, nuclear Overhauser effect spectroscopy (NOESY) revealed correlations between all four distinct protons of pTP and the inner aromatic protons of the nanobelt (Figure 3a,c). This definitively confirms interaction between **1b** and pTP in solution and indicates that, even at low temperatures, the binding is nonspecific, with pTP likely shuttling and rotating significantly within the nanobelt cavity. To quantify the strength of binding, ¹H NMR titration experiments were conducted in benzene-*d*₆, where the guest concentration was held constant while the host concentration was varied over 3 orders of magnitude (Figures S20 and S21). Fitting these curves⁴¹ provided an association constant (K_a) of $54 \pm 1 \text{ M}^{-1}$ for pTP and $148 \pm 3 \text{ M}^{-1}$ for QT. To our knowledge, this is the first instance of a *p*-phenylene or oligothiophene host–guest complex in nonpolar solvent, highlighting the potential value of a fully fused radial π system for supramolecular chemistry. Additionally, the **1b**•QT complex shown here bears resemblance to the carbon nanotube–sexithiophene complex reported by Loi et al.,⁴² suggesting that higher aspect ratio nanobelts may better mimic some behaviors of their parent carbon nanotubes.

In conclusion, the synthetic strategy described above provides a new approach to carbon nanobelt synthesis with several key advantages over current methods, including higher overall yields and scalability, divergent functionalization, and access to new structural features. Most significantly, this synthetic method highlights a general principle for greater efficiency in the assembly of fused macrocycles, which is that highly fused monomeric building blocks offer significant advantages in mitigating the challenges associated with introduction of strain in the construction of fused-ring macrocycles. This strategy has enabled synthesis of a high aspect ratio CNB, whose long, narrow structure facilitates binding of oligo-arylene guests in nonpolar solvents. This unusual affinity points to a new potential application for CNBs in the synthesis of fully conjugated mechanically interlocked molecules and molecular machines. This is the first instance of a CNB performing a unique function not easily attainable by other means and is thus an important step in their development as technologically valuable building blocks for more complex materials.

ASSOCIATED CONTENT

Supporting Information

The Supporting Information is available free of charge at <https://pubs.acs.org/doi/10.1021/jacs.1c04037>.

Experimental procedures and characterization data for all new compounds (PDF)

Accession Codes

CCDC 2078025–2078026 contain the supplementary crystallographic data for this paper. These data can be obtained free of charge via www.ccdc.cam.ac.uk/data_request/cif, or by emailing data_request@ccdc.cam.ac.uk, or by contacting The Cambridge Crystallographic Data Centre, 12 Union Road, Cambridge CB2 1EZ, UK; fax: +44 1223 336033.

AUTHOR INFORMATION

Corresponding Author

T. Don Tilley – Department of Chemistry, University of California, Berkeley, Berkeley, California 94720, United States; orcid.org/0000-0002-6671-9099; Email: tdtilley@berkeley.edu

Authors

Harrison M. Bergman – Department of Chemistry, University of California, Berkeley, Berkeley, California 94720, United States; orcid.org/0000-0001-6482-2837

Gavin R. Kiel – Department of Chemistry, University of California, Berkeley, Berkeley, California 94720, United States; orcid.org/0000-0001-6449-8547

Rex C. Handford – Department of Chemistry, University of California, Berkeley, Berkeley, California 94720, United States; orcid.org/0000-0002-3693-1697

Yi Liu – Molecular Foundry, Lawrence Berkeley National Laboratory, Berkeley, California 94720, United States; orcid.org/0000-0002-3954-6102

Complete contact information is available at: <https://pubs.acs.org/10.1021/jacs.1c04037>

Funding

This work was funded by the National Science Foundation under Grant No. CHE-2103696.

Notes

The authors declare no competing financial interest.

ACKNOWLEDGMENTS

Work performed at the Molecular Foundry was supported by the Office of Science, Office of Basic Energy Sciences, of the US Department of Energy under Contract No. DE-AC02-05CH11231. The computational work was performed at the UC Berkeley Molecular Graphics and Computation Facility (MGCF), which is supported by the National Institute of Health (Grant No. NIH S10OD023532), and the authors thank Dr. Dave Small and Dr. Kathy Durkin for their assistance with these calculations. The authors thank Dr. Hasan Celik for assistance with NMR spectroscopy. Crystallographic analysis was performed at The Advanced Light Source, which is supported by the Director, Office of Science, Office of Basic Energy Sciences, of the U.S. Department of Energy under Contract No. DE-AC02-05CH11231. We thank Dr. Simon Teat (ALS, LBNL) for X-ray crystallography advice.

REFERENCES

- (1) Guo, Q. H.; Qiu, Y.; Wang, M. X.; Stoddart, J. F. Aromatic hydrocarbon belts. *Nat. Chem.* **2021**, *13*, 402–419.
- (2) Cheung, K. Y.; Segawa, Y.; Itami, K. Synthetic Strategies of Carbon Nanobelts and Related Belt-Shaped Polycyclic Aromatic Hydrocarbons. *Chem. - Eur. J.* **2020**, *26*, 14791–14801.
- (3) Zhang, Q.; Zhang, Y. E.; Tong, S.; Wang, M. X. Hydrocarbon Belts with Truncated Cone Structures. *J. Am. Chem. Soc.* **2020**, *142*, 1196–1199.
- (4) Li, Y.; Segawa, Y.; Yagi, A.; Itami, K. A. Nonalternant Aromatic Belt: Methyleno-Bridged [6]Cycloparaphenylenes Synthesized from Pillar[6]Arene. *J. Am. Chem. Soc.* **2020**, *142*, 12850–12856.
- (5) Nishigaki, S.; Shibata, Y.; Nakajima, A.; Okajima, H.; Masumoto, Y.; Osawa, T.; Muranaka, A.; Sugiyama, H.; Horikawa, A.; Uekusa, H.; et al. Synthesis of Belt- And Möbius-Shaped Cycloparaphenylenes by Rhodium-Catalyzed Alkyne Cyclotrimerization. *J. Am. Chem. Soc.* **2019**, *141*, 14955–14960.
- (6) Nogami, J.; Tanaka, Y.; Sugiyama, H.; Uekusa, H.; Muranaka, A.; Uchiyama, M.; Tanaka, K. Enantioselective Synthesis of Planar Chiral Zigzag-Type Cyclophenylene Belts by Rhodium-Catalyzed Alkyne Cyclotrimerization. *J. Am. Chem. Soc.* **2020**, *142*, 9834–9842.
- (7) Xie, J.; Li, X.; Wang, S.; Li, A.; Jiang, L.; Zhu, K. Heteroatom-Bridged Molecular Belts as Containers. *Nat. Commun.* **2020**, *11*, 1–6.
- (8) Zhu, J.; Han, Y.; Ni, Y.; Li, G.; Wu, J. Facile Synthesis of Nitrogen-Doped [(6.0)8]n Cyclacene Carbon Nanobelts by a One-Pot Self-Condensation Reaction. *J. Am. Chem. Soc.* **2021**, *143*, 2716–2721.
- (9) Wang, J.; Miao, Q. A Tetraazapentacene-Pyrene Belt: Toward Synthesis of N-Doped Zigzag Carbon Nanobelts. *Org. Lett.* **2019**, *21*, 10120–10124.
- (10) Neuhaus, P.; Cnossen, A.; Gong, J. Q.; Herz, L. M.; Anderson, H. L. A Molecular Nanotube with Three-Dimensional π -Conjugation. *Angew. Chem., Int. Ed.* **2015**, *54*, 7344–7348.
- (11) Xue, S.; Kuzuhara, D.; Aratani, N.; Yamada, H. Synthesis of a Porphyrin(2.1.2.1) Nanobelt and Its Ability to Bind Fullerene. *Org. Lett.* **2019**, *21*, 2069–2072.
- (12) Standera, M.; Häfliger, R.; Gershoni-Poranne, R.; Stanger, A.; Jeschke, G.; van Beek, J. D.; Bertschi, L.; Schlüter, A. D. Evidence for Fully Conjugated Double-Stranded Cycles. *Chem. - Eur. J.* **2011**, *17*, 12163–12174.
- (13) Esser, B.; Rominger, F.; Gleiter, R. Synthesis of [6.8]-3cyclacene: Conjugated Belt and Model for an Unusual Type of Carbon Nanotube. *J. Am. Chem. Soc.* **2008**, *130*, 6716–6717.
- (14) Sun, Z.; Ikemoto, K.; Fukunaga, T. M.; Koretsune, T.; Arita, R.; Sato, S.; Isobe, H. Finite Phenine Nanotubes with Periodic Vacancy Defects. *Science* **2019**, *363*, 151–155.
- (15) Ikemoto, K.; Yang, S.; Naito, H.; Kotani, M.; Sato, S.; Isobe, H. A Nitrogen-Doped Nanotube Molecule with Atom Vacancy Defects. *Nat. Commun.* **2020**, *11*, 1–6.
- (16) Heilbronner, E. Molecular Orbitals in Homologous Reihen Mehrkerniger Aromatischer Kohlenwasserstoffe: I. Die Eigenwerte Yon LCAO-MO's in Homologen Reihen. *Helv. Chim. Acta* **1954**, *37*, 921–935.
- (17) Kohnke, F. H.; Slawin, A. M. Z.; Stoddart, J. F.; Williams, D. J. Molecular Belts and Collars in the Making: A Hexaepoxyoctacosahydro[12]Cyclacene Derivative. *Angew. Chem., Int. Ed. Engl.* **1987**, *26*, 892–894.
- (18) Godt, A.; Enkelmann, V.; Schlüter, A.-D. Double-Stranded Molecules: A [6]Beltene Derivative and the Corresponding Open-Chain Polymer. *Angew. Chem., Int. Ed. Engl.* **1989**, *28*, 1680–1682.
- (19) Vögtle, F.; Schröder, A.; Karbach, D. Strategy for the Synthesis of Tube-Shaped Molecules. *Angew. Chem., Int. Ed. Engl.* **1991**, *30*, 575–577.
- (20) Iijima, S. Helical Microtubules of Graphitic Carbon. *Nature* **1991**, *354*, 56–58.
- (21) Fort, E. H.; Donovan, P. M.; Scott, L. T. Diels-Alder Reactivity of Polycyclic Aromatic Hydrocarbon Bay Regions: Implications for Metal-Free Growth of Single-Chirality Carbon Nanotubes. *J. Am. Chem. Soc.* **2009**, *131*, 16006–16007.
- (22) Omachi, H.; Nakayama, T.; Takahashi, E.; Segawa, Y.; Itami, K. Initiation of Carbon Nanotube Growth by Well-Defined Carbon Nanorings. *Nat. Chem.* **2013**, *5*, 572–576.
- (23) Sanchez-Valencia, J. R.; Dienel, T.; Gröning, O.; Shorubalko, I.; Mueller, A.; Jansen, M.; Amsharov, K.; Ruffieux, P.; Fasel, R. Controlled Synthesis of Single-Chirality Carbon Nanotubes. *Nature* **2014**, *512*, 61–64.
- (24) Cory, R. M.; McPhail, C. L.; Dikmans, A. J.; Vittal, J. J. Macrocyclic Cyclophane Belts via Double Diels-Alder Cycloadditions: Macroannulation of Bisdienes by Bisdieneophiles. Synthesis of a Key Precursor to an [8]Cyclacene. *Tetrahedron Lett.* **1996**, *37*, 1983–1986.
- (25) Cory, R. M.; McPhail, C. L. Transformations of a Macrocyclic Cyclophane Belt into Advanced [8]Cyclacene and [8]Cyclacene Triquinone Precursors. *Tetrahedron Lett.* **1996**, *37*, 1987–1990.
- (26) Nakamura, E.; Tahara, K.; Matsuo, Y.; Sawamurat, M. Synthesis, Structure, and Aromaticity of a Hoop-Shaped Cyclic Benzenoid [10]Cyclophenacene. *J. Am. Chem. Soc.* **2003**, *125*, 2834–2835.
- (27) Iyoda, M.; Kuwatani, Y.; Nishinaga, T.; Takase, M.; Nishiuchi, T. Conjugated Molecular Belts Based on 3D Benzannulene Systems. In *Fragments of Fullerenes and Carbon Nanotubes*; Petrukhina, M. A., Scott, L. T., Eds.; John Wiley & Sons: 2011; pp 311–342. DOI: [10.1002/9781118011263](https://doi.org/10.1002/9781118011263).
- (28) Shi, T. H.; Guo, Q. H.; Tong, S.; Wang, M. X. Toward the Synthesis of a Highly Strained Hydrocarbon Belt. *J. Am. Chem. Soc.* **2020**, *142*, 4576–4580.
- (29) Povie, G.; Segawa, Y.; Nishihara, T.; Miyauchi, Y.; Itami, K. Synthesis of a Carbon Nanobelt. *Science* **2017**, *356*, 172–175.
- (30) Povie, G.; Segawa, Y.; Nishihara, T.; Miyauchi, Y.; Itami, K. Synthesis and Size-Dependent Properties of [12], [16], and [24] Carbon Nanobelts. *J. Am. Chem. Soc.* **2018**, *140*, 10054–10059.
- (31) Cheung, K. Y.; Gui, S.; Deng, C.; Liang, H.; Xia, Z.; Liu, Z.; Chi, L.; Miao, Q. Synthesis of Armchair and Chiral Carbon Nanobelts. *Chem* **2019**, *5*, 838–847.
- (32) Cheung, K. Y.; Watanabe, K.; Segawa, Y.; Itami, K. Synthesis of a Zigzag Carbon Nanobelt. *Nat. Chem.* **2021**, *13*, 255–259.
- (33) Han, Y.; Dong, S.; Shao, J.; Fan, W.; Chi, C. Synthesis of a Sidewall Fragment of a (12,0) Carbon Nanotube. *Angew. Chem., Int. Ed.* **2021**, *60*, 2658–2662.
- (34) Xia, Z.; Pun, S. H.; Chen, H.; Miao, Q. Synthesis of Zigzag Carbon Nanobelts through Scholl Reactions. *Angew. Chem., Int. Ed.* **2021**, *60*, 10311–10318.
- (35) Kiel, G. R.; Bergman, H. M.; Tilley, T. D. Site-Selective [2 + 2 + n] Cycloadditions for Rapid, Scalable Access to Alkynylated Polycyclic Aromatic Hydrocarbons. *Chem. Sci.* **2020**, *11*, 3028–3035.

(36) Kiel, G. R.; Bay, K. L.; Samkian, A. E.; Schuster, N. J.; Lin, J. B.; Handford, R. C.; Nuckolls, C.; Houk, K. N.; Tilley, T. D. Expanded Helicenes as Synthons for Chiral Macrocyclic Nanocarbons. *J. Am. Chem. Soc.* **2020**, *142*, 11084–11091.

(37) Mysliwiec, D.; Stępień, M. The Fold-In Approach to Bowl-Shaped Aromatic Compounds: Synthesis of Chrysaoroles. *Angew. Chem., Int. Ed.* **2013**, *52*, 1713–1717.

(38) Leonhardt, E. J.; Jasti, R. Emerging Applications of Carbon Nanohoops. *Nat. Rev. Chem.* **2019**, *3*, 672–686.

(39) The only report to date of host–guest chemistry is the complexation of C_{60} by two CNBs reported in ref 34.

(40) Sure, R.; Grimme, S. Comprehensive Benchmark of Association (Free) Energies of Realistic Host-Guest Complexes. *J. Chem. Theory Comput.* **2015**, *11*, 3785–3801.

(41) Thordarson, P. Determining Association Constants from Titration Experiments in Supramolecular Chemistry. *Chem. Soc. Rev.* **2011**, *40*, 1305–1323.

(42) Loi, M. A.; Gao, J.; Cordella, F.; Blondeau, P.; Menna, E.; Bártová, B.; Hébert, C.; Lazar, S.; Botton, G. A.; Milko, M.; et al. Encapsulation of Conjugated Oligomers in Single-Walled Carbon Nanotubes: Towards Nanohybrids for Photonic Devices. *Adv. Mater.* **2010**, *22*, 1635–1639.